

Quantum rotational fluctuation of a linear molecule doped in superfluid helium clusters

This article has been downloaded from IOPscience. Please scroll down to see the full text article.

2008 J. Phys.: Condens. Matter 20 494205

(<http://iopscience.iop.org/0953-8984/20/49/494205>)

View [the table of contents for this issue](#), or go to the [journal homepage](#) for more

Download details:

IP Address: 129.252.86.83

The article was downloaded on 29/05/2010 at 16:44

Please note that [terms and conditions apply](#).

Quantum rotational fluctuation of a linear molecule doped in superfluid helium clusters

Shinichi Miura

Graduate School of Natural Science and Technology, Kanazawa University, Kakuma, Kanazawa 920-1192, Japan

E-mail: smiura@mail.kanazawa-u.ac.jp

Received 31 July 2008, in final form 4 September 2008

Published 12 November 2008

Online at stacks.iop.org/JPhysCM/20/494205

Abstract

Using a path integral hybrid Monte Carlo method, the author examines quantum rotational fluctuation of an OCS molecule in helium-4 clusters as a function of cluster size N : a small-to-large size regime, $2 \leq N \leq 64$. The molecular rotation of the dopant is found to show non-monotonic size dependence in the medium size regime, $10 \leq N \leq 20$, reflecting the onset of the superfluidity and the reconfiguration of the helium density around the molecule. For larger size regime, $N \geq 20$, oscillatory N dependence in the orientational fluctuation and the associated effective rotational constant is found. The oscillation is demonstrated to arise from the effect of the Bose statistics in the cluster by comparing the size dependence with the Boltzmann counterpart.

(Some figures in this article are in colour only in the electronic version)

1. Introduction

In recent years, superfluid helium nanodroplets have attracted a great deal of interest in the field of low temperature chemistry and physics [1–4]. Quantum fluctuation of the medium has been found to have a dramatic impact on chemical processes in the nanodroplet. An impressive example is provided by the rotational dynamics of dopant molecules in the nanodroplets [5]. Spectroscopic measurements on the doped droplets have shown that the solvated molecules rotate freely in an effective manner, arising from the superfluidity of the nanodroplets. Conversely, this indicates the dopant spectroscopy in the helium nanodroplets offers a unique opportunity to probe the properties of quantum fluids at finite size.

Various dopants have been studied both experimentally [1, 2, 5–9] and theoretically [3, 4, 10–23]. Among them, a carbonyl sulfide (OCS) molecule is one of the most widely studied dopants in helium nanodroplets. Recently, Tang *et al* [6] have determined the vibrational and rotational spectra of the OCS(He) $_N$ clusters in a small-to-medium size regime, $N = 2$ –8. They found an effective rotational constant B_{eff} , which is inversely proportional to an effective moment of inertia of the solvated molecule, decreases monotonically as N increases.

The rotational constant for $N = 5$ was found to be almost the same value for the nanodroplet, and then overshoots the nanodroplet limit. Very recently, McKeller *et al* [9] reported detailed size dependence of the effective rotational constant for OCS up to the cluster size $N = 72$. They found that the experimental B_{eff} shows unexpected oscillatory behavior in a medium-to-large size regime, $N > 20$, which does not reach the nanodroplet limit yet.

From a theoretical viewpoint, the size dependence on the rotational fluctuation of the OCS molecule has been studied by ground-state quantum Monte Carlo (QMC) techniques for clusters in the small-to-medium size regime [13, 14]. The calculations predicted a minimum in the N -dependent rotational constant at $N = 8$ –9 [14] or $N = 6$ [13]; the small discrepancy between the calculations presumably arises from the difference in the He–OCS interaction adopted. Then, the constant increase of B_{eff} was found up to $N = 20$. At a finite temperature corresponding to the experimental condition, a path integral Monte Carlo (PIMC) technique has been applied to a fixed classical OCS molecule dissolved in the helium clusters [3, 11]. Recently, we have developed a path integral hybrid Monte Carlo (PIHMC) method to handle the rotational motion of the dopant molecules quantum-mechanically [20].

Then, the PIHMC was applied to the OCS-doped helium-4 cluster to study the impact of the Bose statistics on the rotational correlation in the solvated molecule. Independently, Zillich *et al* [18] and Blinov and Roy [19] have developed a PIMC method to treat rotating molecules in superfluids and applied the method to the OCS-doped helium cluster. In this paper, the size dependence of the rotational fluctuation of the OCS molecule is systematically studied by the PIHMC method in the small-to-large size regime, $N = 2$ –64. In particular, special attention is paid to the medium-to-large size regime where the rotational fluctuation has not been well studied theoretically to resolve the above-mentioned oscillation in the rotational constant.

2. Method

Here, we summarize the PIHMC method for doped quantum clusters. We consider the system consisting of N helium-4 atoms obeying Bose–Einstein statistics and an OCS molecule modeled as a rigid rotor. The partition function of the system Z at an inverse temperature $\beta = 1/k_B T$ is written in discretized path integral form as [24, 25]

$$Z = \frac{1}{N!} \sum_{\mathcal{P}} \int \cdots \int \prod_{s=1}^M d\mathbf{R}^{(s)} d\Omega^{(s)} \times \prod_{s=1}^M \rho(\mathbf{R}^{(s)}, \Omega^{(s)}, \mathbf{R}^{(s+1)}, \Omega^{(s+1)}; \Delta\tau), \quad (1)$$

where $\Delta\tau = \beta/M$ is the imaginary time step and $\rho(\Delta\tau)$ is the short time (or high temperature) density matrix of the system. Here, $\mathbf{R}^{(s)}$ denotes the $3(N+1)$ -dimensional position vector including the molecule’s center-of-mass position and $\Omega^{(s)}$ represents the molecule’s orientation in the laboratory frame; the superscript s runs from 1 to M , labeling the imaginary time slice. The permutation \mathcal{P} is included in the boundary condition of the path as $\mathbf{R}^{(M+1)} = \mathcal{P}\mathbf{R}^{(1)}$. In the present study, the He–He contribution in the density matrix is represented using the pair-product form of the exact two-body density matrices [24] and the He–molecule contribution is approximated using the standard factorization technique accurate up to $\mathcal{O}(\Delta\tau^4)$ [25]. In the latter expression, the rotational density matrix of the molecule is included as [25]

$$\rho^{\text{rot}}(\Omega^{(s)}, \Omega^{(s+1)}; \Delta\tau) = \sum_{J=0}^{\infty} \frac{2J+1}{4\pi} P_J(\cos\gamma) e^{-\Delta\tau B J(J+1)}, \quad (2)$$

where P_J is a Legendre function and γ is an angle between the molecular axis of two successive time slices. The parameter B is the rotational constant of the molecule related to the moment of inertia I , $B = \hbar^2/2I$. In order to incorporate the molecular rotation in the hybrid Monte Carlo algorithm, we define the following ‘potential function’ using the rotational density matrix: $\rho^{\text{rot}}(\Delta\tau) \equiv e^{-\Delta\tau W^{\text{rot}}(\Omega, \Omega)}$. We refer to W^{rot} as an effective potential of quantum rotation [20, 21]. In the hybrid Monte Carlo, an equation of motion is needed to generate trial configurations. We introduce a fictitious angular momentum and a fictitious moment of inertia to sample rotational fluctuations. Then, we integrate this technique

into our hybrid Monte Carlo algorithms for correlated Bose fluids [26]. Full details of the method can be found elsewhere [21].

3. Computational details

The calculated system consists of N helium-4 atoms and an OCS molecule. The cluster size studied ranges from the small to large cluster regime: $N = 2$ –12, 15, 20, 30, 40, 50 and 64. The temperature of the system was controlled to be 0.37 K. The number of discretizations needed for the path integral expression was chosen to be $M = 216$, corresponding to $1/\Delta\tau = 80$ K. The rotational constant of the OCS molecule was taken from a gas-phase experimental value $B_{\text{OCS}} = 0.20286 \text{ cm}^{-1}$ [27] to construct the effective potential of quantum rotation on a fine grid. The Aziz potential [28] was used as a pairwise interaction between two helium atoms. The pair density matrix of helium-4 atoms was evaluated numerically by a matrix squaring technique [24], which defines the effective interaction among the helium-4 atoms [26, 29]. The morphed potential of Howson and Hutson [30] was adopted for the He–OCS interaction. Path integral hybrid Monte Carlo calculations were performed for the system obeying Bose–Einstein statistics. For comparison, the systems obeying Maxwell–Boltzmann statistics were also examined.

4. Results

Prior to presenting the results of the rotational fluctuation of the OCS molecule, we first summarize the size dependence of the helium density distribution around the molecule and the effect of the Bose statistics on the density distribution. Selected results can be found in [22]. At $N = 5$, all the helium atoms are localized around the C atom where the He–OCS interaction is a minimum, forming a donut-type structure of the density around the molecular axis. Then, the helium atoms start to populate around other potential minima located near the O and S atoms with increasing N . At $N = 10$, the helium distribution is found in the whole region in the vicinity of the molecule. For $N > 10$, density augmentation is observed in the intermediate region between the S and C atoms in the first solvation shell, making a new peak of the density distribution. For $N > 15$, the addition of the helium atoms induces the reconfiguration of the solvation shell; the peak near the S atom becomes lowered and shifted in the direction of the C atom along the solvation shell. At $N = 20$, the first solvation shell is nearly completed. For $N > 20$, the second solvation shell starts to be filled by the helium, accompanied by the density increase in the first solvation shell up to $N = 64$. The trend found in the size dependence of the density distribution is common to both the Bose and Boltzmann clusters; the Bose statistics makes the density distribution slightly broader. To extract the effect of the Bose statistics, we decompose the density profile on the basis of the length of the exchange cycles. At $N = 5$, the five-body exchange cycles are observed to a large extent; in this case, the contributions from the two- to four-body cycles are negligible. These exchange cycles are located around the

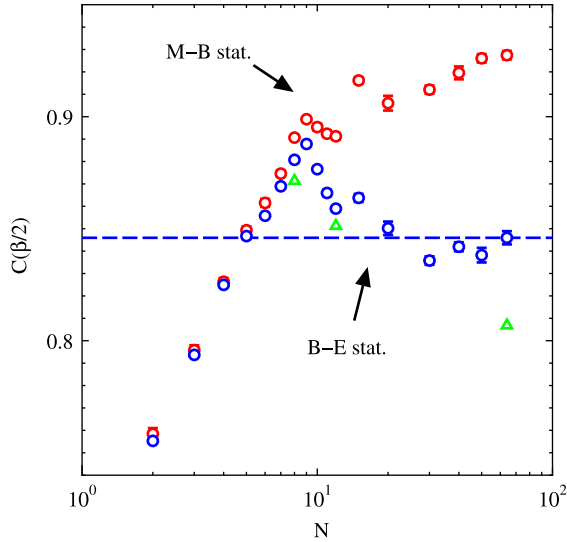


Figure 1. The imaginary time orientational correlation function of the OCS at the imaginary time $\beta/2$ as a function of the cluster size N . Blue open circles are for the Bose clusters and red open circles for the Boltzmann clusters. Dashed line indicates the $C(\beta/2)$ value for $N = 64$. Green open triangles represent the $C(\beta/2)$ values by path integral Monte Carlo calculations of the Bose clusters doped with the OCS molecule [18]. The error bar is expressed at 95% confidence level and is smaller than the size of the corresponding data symbol when it is not shown.

molecular axis in the donut structure. For $6 \leq N \leq 9$, the long-exchange cycles start to be observed in the region over the C and O atoms. At $N = 10$, the bosonic exchange between the C and S regions starts to become visible, indicating the exchange cycles of the helium atoms are present to wrap the OCS molecule in the plane including the molecular axis. This type of configuration triggers the superfluidity of the doped clusters [22]. With further increasing N , the contribution from the long-exchange cycles becomes larger. For $N \geq 20$, the long-exchange cycles give the dominant contribution in the density distribution. While the helium density around the molecule increases constantly with N , the contribution from the non-exchange and short-exchange cycles decreases monotonically up to $N = 64$.

We show the cluster size dependence of the rotational fluctuation of the dopant molecule. The rotational fluctuation can be probed by the following orientational correlation function in imaginary time:

$$C(\tau) = \langle \mathbf{e}(\tau) \cdot \mathbf{e}(0) \rangle. \quad (3)$$

where $\mathbf{e}(\tau)$ is a unit vector of the molecular axis at the imaginary time τ . The rotational fluctuation of the molecule can be characterized by $C(\tau)$ at $\tau = \beta/2$. Full time dependence of $C(\tau)$ can be found, for example, in [20, 21]. Since $\mathbf{e}(\tau) \cdot \mathbf{e}(0) = \cos \gamma(\tau)$, where $\gamma(\tau)$ is an angle between $\mathbf{e}(\tau)$ and $\mathbf{e}(0)$, the smaller $C(\beta/2)$ value indicates a larger orientational fluctuation. The $C(\beta/2)$ can be written for a free OCS in an analytical form [31]:

$$C(\beta/2) = \frac{\sum_{J>0} 2J e^{-\beta B_{\text{OCS}} J^2}}{Z}, \quad (4)$$

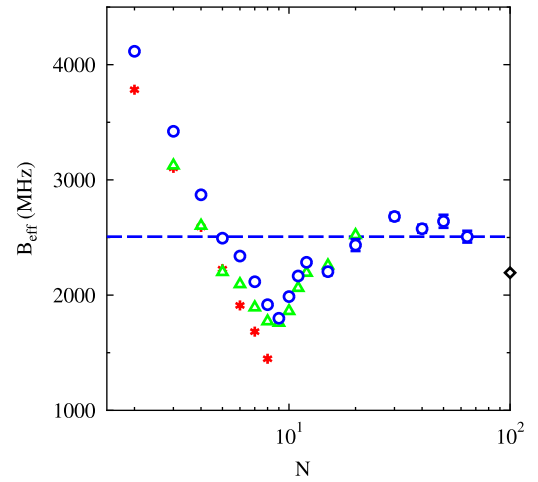


Figure 2. The effective rotational constant B_{eff} as a function of the cluster size N . Blue open circles represent the estimated values for Bose clusters and green open triangles B_{eff} by the ground-state quantum Monte Carlo calculations [14]. Star symbols show the experimental B_{eff} reported in [6]. Open diamond indicates the experimental nanodroplet value [32]. The dashed line indicates the B_{eff} value of $N = 64$. The error bar is estimated so as to be consistent with the statistical error of $C(\beta/2)$ in figure 1.

where $Z = \sum_{J \geq 0} (2J + 1) e^{-\beta B_{\text{OCS}} J(J+1)}$. Figure 1 shows the size-dependent $C(\beta/2)$ of the OCS molecule in the Boltzmann and Bose clusters. The Boltzmann $C(\beta/2)$ monotonically increases with N (≤ 9) and reaches a maximum at $N = 9$. A second maximum in the size dependence is found at $N = 15$. For $N \geq 20$, the $C(\beta/2)$ value again increases monotonically up to $N = 64$. On the other hand, the Bose $C(\beta/2)$ first increases with N (≤ 5) where the effect of the Bose statistics is negligible. Then, the Bose $C(\beta/2)$ starts to deviate from the Boltzmann $C(\beta/2)$ with N , indicating the rotational fluctuation becomes larger than that of the OCS molecule doped in the Boltzmann cluster. In the size range $N \geq 10$, the effect of the Bose statistics becomes remarkable; the magnitude of the $C(\beta/2)$ is much reduced compared with the Boltzmann counterpart, which is directly connected to the onset of the superfluidity of the doped cluster, although the presence of the two peaks in the range $N \leq 20$ is a common feature of the Bose and Boltzmann clusters. For $N \geq 20$, the $C(\beta/2)$ is found to show oscillatory size dependence, showing clear contrast with the Boltzmann cluster where the $C(\beta/2)$ increases monotonically. Here, we comment on the PIMC calculations of the $\text{OCS}({}^4\text{He})_N$ clusters for $N = 8, 12$ and 64 by Zillich *et al* [18]. Although the size dependence on $C(\beta/2)$ by their calculations shows a similar trend with our calculations for the selected cluster sizes, the rotational fluctuation of the OCS molecule for $N = 64$ by their calculation is much larger than that by our calculation. This can be partly ascribed to the difference in the He–OCS interaction adopted.

Next, we estimate the effective rotational constant B_{eff} of the solvated molecule using the above $C(\beta/2)$ value. The estimation procedure is the same as that presented in [21] using the calculated $C(\beta/2)$ value and the analytical expression of $C(\beta/2)$, equation (4). Figure 2 shows the estimated effective rotational constant B_{eff} as a function of N , together with

the experimental data [6, 32] and the reported ground-state quantum Monte Carlo values [14]. The effective rotational constant by the present study decreases with increasing N up to 9, and then shows a turnover. We find a second (weak) minimum at $N = 15$ corresponding to the second maximum in the size dependence on $C(\beta/2)$. For $N \geq 20$, the effective rotational constant shows oscillatory size dependence. At the largest cluster examined in this study $N = 64$, the estimated rotational constant can still be larger than the experimental nanodroplet value. Our estimated B_{eff} values are in good agreement with the experimental B_{eff} by Tang *et al* [6]. Also good agreement of the present results with the QMC values is found up to $N = 20$. The oscillatory size dependence found in the medium-to-large size regime is in good accordance with the very recent experimental results by McKellar *et al* [9] who reported the experimental effective rotational constant of the OCS in the helium cluster up to $N = 72$. They found that the experimental B_{eff} shows oscillatory behavior in the medium-to-large size regime, $N > 20$, which does not reach the nanodroplet limit yet. To our knowledge, in the present study, the oscillatory size dependence is theoretically reproduced for the first time. Since, as shown above, the rotational fluctuation has monotonic size dependence for the Boltzmann cluster in the range $N \geq 20$, the oscillatory behavior found in B_{eff} arises from the bosonic nature of the cluster.

5. Concluding remarks

In this paper, we have examined the rotational fluctuation of the OCS molecule in helium-4 clusters for $2 \leq N \leq 64$ using the path integral hybrid Monte Carlo method. A remarkable enhancement of the molecular rotation in the Bose cluster is found for $N \geq 10$, being connected to the onset of superfluidity. We also find the rotational fluctuation and the associated effective rotational constant show non-monotonic size dependence in the medium size regime $10 \leq N \leq 20$. For the medium-to-large size regime, $20 \leq N \leq 64$, the effective rotational constant of the molecule in the Bose cluster shows oscillatory size dependence, which is in good correspondence with the experimental results by McKellar *et al* [9] who interpreted the oscillation as a manifestation of the *aufbau* of a nonclassical helium solvation shell structure. Although, in this paper, the oscillation is demonstrated to come from the effect of the Bose statistics in the cluster, molecular detail has not been well clarified yet. This issue will be addressed in a future study.

Acknowledgments

This work was partially supported by the Grant-in-Aid for Scientific Research (no. 19550026) from the Japan Society for

the Promotion of Science and by the Next Generation Super Computing Project, Nanoscience Program, MEXT, Japan.

References

- [1] Toennies J P and Vilesov D F 1998 *Annu. Rev. Phys. Chem.* **49** 1 and references therein
- [2] Toennies J P and Vilesov D F 2004 *Angew. Chem. Int. Edn* **43** 2622 and references therein
- [3] Kwon Y, Huang P, Patel M V, Blume D and Whaley K B 2000 *J. Chem. Phys.* **113** 6469 and references therein
- [4] Barranco M, Guardiola R, Hernández S, Mayol R, Navarro J and Pi M 2006 *J. Low Temp. Phys.* **142** 1 and references therein
- [5] Grebenev S, Toennies J P and Vilesov A F 1998 *Science* **279** 2083
- [6] Tang J, Xu Y, McKellar A R W and Jäger W 2002 *Science* **297** 2030
- [7] Xu Y, Jäger W, Tang J and McKellar A R W 2003 *Phys. Rev. Lett.* **91** 163401
- [8] Tang J, McKellar A R W, Mezzacapo F and Moroni S 2004 *Phys. Rev. Lett.* **92** 145503
- [9] McKellar A R W, Xu Y and Jäger W 2006 *Phys. Rev. Lett.* **97** 183401
- [10] Kwon Y and Whaley K B 1999 *Phys. Rev. Lett.* **83** 4108
- [11] Kwon Y and Whaley K B 2001 *J. Chem. Phys.* **115** 10146
- [12] Draeger E W and Ceperley D M 2003 *Phys. Rev. Lett.* **90** 065301
- [13] Paesani F, Viel A, Gianturco F A and Whaley K B 2003 *Phys. Rev. Lett.* **90** 073401
- [14] Moroni S, Sarsa A, Fantoni S, Schmidt K E and Baroni S 2003 *Phys. Rev. Lett.* **90** 143401
- [15] Moroni S, Brinov N and Roy P-N 2004 *J. Chem. Phys.* **121** 3577
- [16] Paesani F and Whaley K B 2004 *J. Chem. Phys.* **121** 4180
- [17] Paolini S, Fantoni S, Moroni S and Baroni S 2005 *J. Chem. Phys.* **123** 114306
- [18] Zillich R E, Paesani F, Kwon Y and Whaley K B 2005 *J. Chem. Phys.* **123** 114301
- [19] Blinov N and Roy P-N 2005 *J. Low Temp. Phys.* **140** 253
- [20] Miura S 2005 *J. Phys.: Condens. Matter* **17** S3259
- [21] Miura S 2007 *J. Chem. Phys.* **126** 114308
- [22] Miura S 2007 *J. Chem. Phys.* **126** 114309
- [23] Miura S 2007 *J. Low Temp. Phys.* **148** 839
- [24] Ceperley D M 1995 *Rev. Mod. Phys.* **67** 279 and references therein
- [25] Marx D and Muser M H 1999 *J. Phys.: Condens. Matter* **11** R117 and references therein
- [26] Miura S and Tanaka J 2004 *J. Chem. Phys.* **120** 2160
- [27] Hunt N, Foster S C, Johns J W C and McKellar A R W 1985 *J. Mol. Spectrosc.* **111** 42
- [28] Aziz R A, Janzen A R and Moldover M 1995 *Phys. Rev. Lett.* **74** 1586
- [29] Miura S and Okazaki S 2001 *J. Chem. Phys.* **115** 5353
- [30] Howson J M M and Hutson J M 2001 *J. Chem. Phys.* **115** 5059
- [31] Blinov N, Song X G and Roy P-N 2004 *J. Chem. Phys.* **120** 5916
- [32] Grebenev S, Hartmann M, Havenith M, Sartakov B, Toennies J P and Vilesov A F 2000 *J. Chem. Phys.* **112** 4485